Diffusivity of Light Hydrocarbons into Hydrogen

T.-C. Chu, Patsy S. Chappelear, and Riki Kobayashi[1]
Department of Chemical Engineering, William Marsh Rice University, P.O. Box 1892, Houston, Tex. 77001

The trace dispersion method was used to determine infinite dilution diffusion coefficients for the light hydrocarbons methane, ethane, propane, and *n*-butane into hydrogen. The four systems were investigated at two to four temperatures each (−25°, 0°, 25°, and 50°C) at maximum pressures up to 150–500 psia. Replacement of the thermal conductivity detector by a microionization chamber enabled measurements on CH_3T into hydrogen at 25°C up to 1100 psia. The experiments were made at various laminar flow rates to insure that spurious effects were not introduced. The data were analyzed by both the single flow rate and multiflow rate methods. A high-pressure slug injection valve was designed to give a slug injection as required by the theoretical model.

Experimental data on dilute gas mixtures of hydrogen and light hydrocarbons are scarce and are tabulated in Table I.

All previous investigations reported in Table I used the Loschmidt method at 1 atm and 25°C. All measurements reported here were at higher pressures and various temperatures. Comparison can be made using the ρD = constant obtained at 25°C and interpreted at 1 atm. These results are 3.8% higher for $CH_4^\infty \rightarrow H_2$, 4.4% higher for $C_2H_6^\infty \rightarrow H_2$, and 5% higher for $C_3H_8^\infty \rightarrow H_2$. This is well within the 5–10% experimental accuracy of the earlier investigations.

The results of this work have an accuracy of 1%; many recent investigations (*1–5, 7–9, 12, 16, 17, 20, 21, 26, 27*) have shown that the trace dispersion method is superior to the Loschmidt method.

In addition, the validity of these results is substantiated by the recent thesis of Chuang (*14*) on viscosity. His correlation predicted D_{12} values consistent with those obtained here.

Previous Use of Method

The trace dispersion method has been used and studied by Taylor (*26, 27*), Aris (*3, 4*), and Balenovic et al. (*6*). Chang and Kobayashi (*11, 12*) studied the He–N_2, CH_4–C_2H_6, CH_4–*n*-C_4H_{10} systems at dilute and moderate densities. Hu and Kobayashi (*17*) studied the conditions under which measurements could be carried out for the He–CH_4, He–N_2, He–Ar, and He–CO_2 systems. The dispersion method using a thermal conductivity (TC) detector with extension to the isotopic system ^{4}He–^{3}He was recently conducted by Liner and Weissman (*22*).

Knox and McLaren (*19*) used an "arrested elution method." The method consists of the injection of a thin band of a nonadsorbed solute into a column and the elution at a controlled and measured velocity. When the band is about half way down the column, the flow is arrested and the band is allowed to spread by diffusion for different times. The band is then eluted from the column, and its concentration profile is determined by a suitable gas chromatographic detector.

Walker et al. (*28–30*) used a "point source technique." The method makes use of the steady injection of a trace gas from a fine hypodermic tube into a slow, uniform, laminar stream of a second (carrier) gas. Measurements of the trace gas concentration downstream of the source, by means of precise gas sampling, permit the binary diffusion coefficients to be determined. By heating the carrier gas the measurements may be extended to fairly high temperatures. They carried out work on the He–N_2, CO_2–N_2, and CO_2–H_2–N_2 systems.

An extensive review of other experimental methods is included in the thesis (*13*) on this work.

Experimental Method and Equipment

This investigation used the trace dispersion method. The details of the equipment, method, and calculations have been reported by Chang and Kobayashi (*11, 12*) and by Hu and Kobayashi (*18*). Only modifications are presented here.

Diffusion tubes. The empty tubes used in this study were made of ⅛-in. o.d. 3/32-in. i.d., with ±0.001-in. tolerance, type 304 SS tubing purchased from J. Bishop Co., Malver, Pa. The tubes were thoroughly cleaned sequentially with benzene, acetone, and ethyl ether to remove

Table I. Previous Experimental Studies on Diffusion in Hydrogen-Hydrocarbon Systems

Year	Name	Method	System	*D*, cm²/sec	*T*	*P*
1880	Obermayer (*24*)	Loschmidt method (*23*)	H_2–CH_4	0.729	25°C	1 atm
			H_2–C_2H_6	0.535	25°C	1 atm
1951	Boyd et al. (*10*)	Interferometric method	H_2–CH_4	0.726	25°C	1 atm
		(Loschmidt-type cell)	H_2–C_2H_6	0.537	25°C	1 atm
1953	Strehlow (*25*)	Hot wire technique	H_2–n-C_4H_{10}	0.361	287.9K	760 mm Hg
		(Loschmidt-type cell)		0.507	354.2K	760 mm Hg
				0.763	430.0K	760 mm Hg
1961	Fejes and Czárán (*15*)	Fluid dispersion in empty tube with tungsten wire as detector	H_2–CH_4	0.73	25°C	1 atm
			H_2–C_2H_6	0.54	25°C	1 atm
			H_2–C_3H_8	0.44	25°C	1 atm
			H_2–n-C_4H_{10}	0.40	25°C	1 atm

---

[1] To whom correspondence should be addressed.

all foreign matter. The short correction diffusion tube and the long diffusion tube were cut from the same coil of tubing, and their ends were finished with a burring tool to remove burrs, etc. The tubes were then coiled to give a 5½-in. o.d. coil. The cross-sectional area of the tube was determined by the retention time method. The tube retention volumes were about 7.8 and 36 cc.

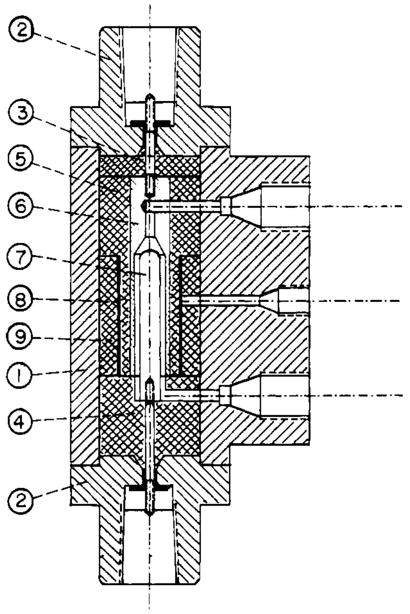

Figure 1. Ionization chamber

	Material
1. Body	303 SS
2. End closure	303 SS
3. Top seal	Teflon
4. Bottom seal	Teflon
5. Inner insulating sleeve	Teflon
6. Outer electrode	303 SS
7. Inner electrode	303 SS
8. Capacitor sleeve	304 SS foil
9. Outer insulating sleeve	Teflon

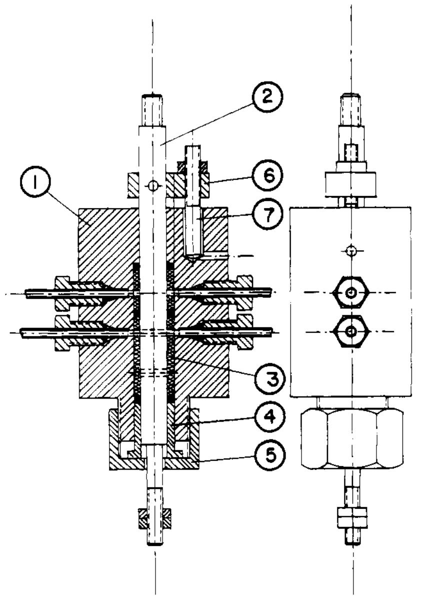

Figure 2. Injection valve

	Material
1. Body	416 SS
2. Plunger	303 SS
3. Packing	Teflon "O" rings
4. Compression sleeve	416 SS
5. Packing nut	416 SS
6. Plunger stop	416 SS
7. Adjusting screw for 6	416 SS

These tubes were from the same lot used in earlier studies in this laboratory by Chang (*11*) and Hu (*17*).

Ionization chamber (IC) detector system. Commercially designed IC cells with a volume usually around 250 cc frequently have a problem of tailing. A microvolume (0.070 cc) IC shown in Figure 1 was designed and built at Rice University to eliminate this problem. Its body was made from 303 SS.

Teflon seals and a spacer made from Kel-F were used. The surfaces of the two electrodes were polished to as high a degree as possible to have a uniform electric field. The sensing volume of this detector was about 70 μl. The electrodes were surrounded with a grounded shield which eliminated electronic noise caused by bath fluid circulation, α-particles, or other causes. A perfect base line was obtained with a noise level less than 10^{-15} amp.

A Cary-31 vibrating reed electrometer was used to measure the current above 10^{-15} amp. The voltage across the electrodes was supplied by a regulated dc unit made by Kepco, Inc., Flushing, N.Y. The output of the dc unit was kept at 12 V.

Sample injection valve. Investigations with the TC detector were made using a 10-μl injection valve rated to 1000 psi manufactured by Micro-Tek Instrument, Inc., Baton Rouge, La. The results above 700 psi appeared to be inconsistent, so a new valve (Figure 2) was designed for a Perfect-Slug injection. The problem was not solved, however, until the IC detector was designed. The new valve was used in the IC investigations.

Radioactive sample pump and store box. To avoid any radioactive release to the open air, the reservoir pump was used. When high pressure was needed, the pump was used to establish the pressure. For low-pressure operation, the pump piston was withdrawn to store the radioactive sample inside the pump. Cylinders containing the radioactive material and the pump were enclosed in a frame and curtain arrangement with a vent. An exhaust fan was operated at all times over the radioactive samples.

Error Analysis

A complete error analysis is based on both the physical aspects of the experimental apparatus and the mathematical methods of computation. Reproducibility gives an indication of the quality of the experimental method and the skill of the experimenter, which are not subject to direct measurement.

Pressure. Heise gages of 300, 500, and 2000 psi ranges were used to measure pressure with an accuracy certified by the manufacturer as 0.1% of full scale. The maximum uncertainty occurs at the lowest pressures: at 25 psia the error is 1.2%; at 50 psia, 0.6%; at 100 psia, 0.3%.

Temperature. The temperature was measured and controlled to ±0.01°, which at −25°C gives an error of 0.004% in temperature.

Flow rate. The diameter of the pistons in the tandem proportioning pump was 2.8089–2.8095 in., which gives a variation of 0.0356% in the flow rate. Other variations could arise if the line current fluctuated, which did not occur; or if the driving gear train were nonuniform. A check on the gear train was made by observation of the displacement of a 1/1000-in. dial indicator micrometer; no shifts were observed.

Retention time. The total elapsed time from sample injection to the peak height was measured by the sum of two values. A mechanical push-button timer was started when the sample was injected. The recorder paper was started just prior to emergence of the peak, and a tic mark was made on the paper when the mechanical timer was stopped. The chart speed and the length from the tic mark to the peak gave the second portion of the total time. The error in the timer is 0.1 sec; in the chart time it is 0.001 sec. The physical layout of the equipment always required the use of the timer. Total residence time ranged from 72 to 4330 sec with most values around 500 sec. The net variation in residence time was estimated to be 0.1%.

Peak width. A Vernier Caliper with an accuracy of 0.001 in. made by the Brown-Sharpe Co., Switzerland, was used. Operator error is estimated as three times the instrument error, or 0.003 in. The reproducibility of the peaks had a large error, 0.5%.

Size of diffusion tube. The tolerance in the radius was specified by the manufacturer as ±0.001 cm. The radius, as determined by the retention time method, was 0.1191 ± 0.001 cm, for an error of 0.8%.

Table II. Summary of Error Analysis

Variable	Estd accuracy of measurement	Resulting variance in D
Pressure	0.1-1.2%	0.2%
Temperature	±0.01°	Nil
Flow rate	0.0356%	Nil
Residence time	0.1%	0.1%
Peak width	0.5%	0.5%
Radius of tube	0.8%	Nil

Table III. Experimental Results for $CH_4^\infty \rightarrow H_2$

Temp, °C	Press, psia	Diffusivity,[a] cm²/sec	Diffusivity,[b] cm²/sec	Density of H_2, g/cc × 10^4
−25	300	0.02734		19.96
	200	0.04027		13.36
	100	0.08008		6.712
	50	0.1559		3.363
0	500	0.01931	0.01964	29.98
	300	0.03262		18.14
	200	0.04795		12.15
	100	0.09465		6.098
	50	0.1899		3.056
25	500	0.02289		27.49
	300	0.03759	0.03759	16.63
	100	0.1114		5.588
50	500	0.02646		25.38
	300	0.04335		15.35
	200	0.06510		10.27
	100	0.1281	0.1276	5.155

Detailed example of results at 25°C and 300 psia

Flow rate, cc/hr	Diffusivity Single flow, cm²/sec	 Multiflow, cm²/sec	Dev, %
40.0	0.03756	0.03759	1
50.0	0.03735		
60.0	0.03766		
80.0	0.03766		
100.0	0.03753		
100.0	0.03760		
100.0	0.03615		
100.0	0.03750		
100.0	0.03741		
120.0	0.03770		
140.0	0.03763		
160.0	0.03800		

[a] Average of single flow rate calculations. [b] Multiflow rate calculation.

Table IV. Experimental Results for $C_2H_6^\infty \rightarrow H_2$

Temp, °C	Press, psia	Diffusivity,[a] cm²/sec	Diffusivity,[b] cm²/sec	Hydrogen density, g/cc × 10^4
0	350	0.02071		21.12
	300	0.02398		18.14
	200	0.03552		12.15
	100	0.07090	0.07077	6.098
25	500	0.01677	0.01694	27.49
	300	0.02776	0.02746	16.63
	100	0.08273		5.588
50	500	0.01989	0.01965	25.38
	300	0.03218		15.35
	200	0.04765		10.27
	100	0.09528	0.09716	5.155

[a] Average of single flow rate calculations. [b] Multiflow rate calculation.

Table V. Experimental Results for $C_3H_8^\infty \rightarrow H_2$

Temp, °C	Press, psia	Diffusivity,[a] cm²/sec	Diffusivity,[b] cm²/sec	Hydrogen density, g/cc × 10^4
0	150	0.04022		9.128
	100	0.05946	0.05918	6.098
	75	0.07877		4.579
	50	0.1181		3.056
	25	0.2370	0.2341	1.529
25	300	0.02293		16.63
	250	0.02780		13.89
	200	0.03510		11.13
	150	0.04695		8.364
	100	0.06995	0.06884	5.588
	75	0.09100	0.09013	4.195
	50	0.1370	0.1340	2.799
	25	0.2711	0.2730	1.401
50	300	0.02707		15.35
	250	0.03251		12.81
	200	0.03961		10.27
	150	0.05387		7.718
	100	0.07909	0.07874	5.155
	75	0.1051		3.870
	50	0.1606	0.1610	2.583
	25	0.3186	0.3098	1.293

[a] Average of single flow rate calculations. [b] Multiflow rate calculation.

Table VI. Experimental Results for $n\text{-}C_4H_{10}^\infty \rightarrow H_2$

Temp, °C	Press, psia	Diffusivity,[a] cm²/sec	Diffusivity,[b] cm²/sec	Hydrogen density, g/cc × 10^4
25	300	0.02077		16.63
	250	0.02519	0.02453	13.89
	200	0.03126		11.13
	150	0.04104		8.364
	100	0.06221		5.588
	50	0.1219		2.799
	30	0.2095	0.2075	1.681
	15	0.4143		0.8410
50	300	0.02450		15.35
	250	0.03048		12.81
	200	0.03605		10.27
	150	0.04890		7.718
	100	0.07273		5.155
	50	0.1436		2.583
	30	0.2425		1.551

[a] Average of single flow rate calculations. [b] Multiflow rate calculation.

Calculation of diffusion coefficient. The primary computation was made according to Equation 1 below. The total error in D is summarized in Table II. The error in the peak width measurement is the predominant factor. The difference of the measurements on the short and long tubes is used, which increases the error. The long tube was approximately four times the length of the short tube, and the square of the width at half height is proportional to the length of the tube. The maximum error in D is 1%.

Calculation of Results

The derivation of the working equations has been reported by Hu and Kobayashi (*18*) for diffusion studies made with a set of long and short diffusion tubes as

$$\frac{\Delta\sigma^2}{\Delta t} = \frac{2}{\bar{u}^2} D + \frac{r_0^2}{24\,D} \tag{1}$$

for some length $L > L_0$, where L_0 is some minimum length so that the response will now show any injection effect, entrance effect, etc.

$\Delta\sigma^2$ = difference in the variance for the long and short tubes, where σ^2 is defined from:

$$W_i^2 = -8(\sigma^2 + a) \ln y_i \text{ for the TC cell detector} \tag{2}$$

$$W_i^2 = -8(\sigma^2 + c) \ln y_i \text{ for the IC cell detector} \tag{3}$$

where W_i is peak width at height y_i, and a and c are constants.

The difference at half peak height is then

$$\Delta W_{1/2}^2 = 8\,\Delta\sigma^2 \ln 2$$

so that $\Delta\sigma^2$ is easily obtained from direct measurements of the width at half peak height, and Δt = difference in residence time for the long and short tubes.

The average velocity of the carrier gas $\bar{u}$ can be experimentally varied, and the radius r_0 of the diffusion tube can be measured. For a single flow rate calculation, D is calculated directly from Equation 1. For a multiple flow rate analysis, a plot of $\Delta\sigma^2/\Delta t$ vs. $2/\bar{u}^2$ will have a slope of D and an intercept of $r_0^2/24\,D$. Consistent results

Table VII. Experimental Results for $CH_3T^\infty \rightarrow H_2$ at 25°C

Press, psia	Flow rate, cc/hr	Diffusivity,^{b} cm²/sec	Diffusivity,^{b} cm²/sec	Hydrogen density, g/cc × 10⁴
1100	15.0	0.01052		59.04
1100	20.0	0.01072		59.04
1100	25.0	0.01056	0.01045	59.04
900	20.0	0.01272		48.69
900	25.0	0.01287	0.01243	48.69
700	25.0	0.01633		38.18
700	30.0	0.01649	0.01597	38.18
500	30.0	0.02292		27.49
500	40.0	0.02300		27.49
500	50.0	0.02260	0.02304	27.49
300	40.0	0.03682		16.63
300	50.0	0.03579		16.63
300	60.0	0.03736		16.63
300	80.0	0.03705		16.63
300	100.0	0.03674		16.63
300	120.0	0.03779		16.63
300	140.0	0.03763	0.03676	16.63
100	140.0	0.1128		5.588
100	160.0	0.1130		5.588
100	200.0	0.1127	0.1129	5.588

^{a} Single flow rate calculation at flow rate indicated. ^{b} Multiflow rate calculation.

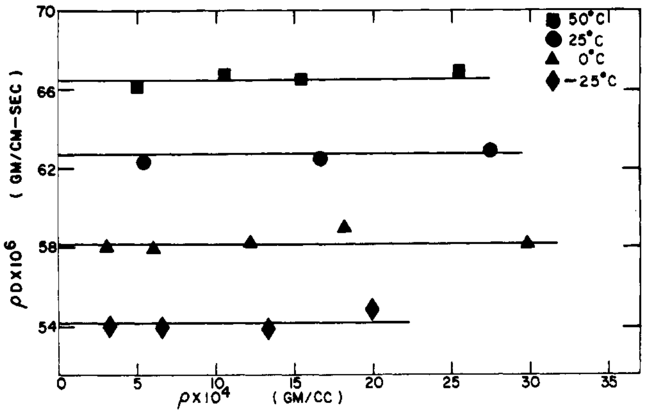

Figure 3. Density-diffusivity product vs. density. Example shown for $CH_4^\infty \rightarrow H_2$ system

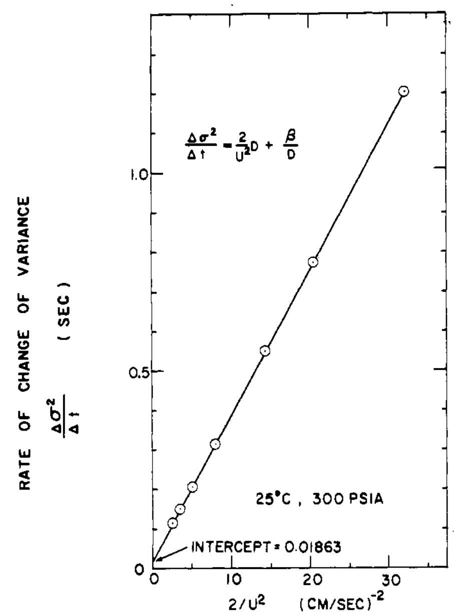

Figure 4. Multiflow perturbation technique for diffusivity. Example shown for $CH_3T^\infty \rightarrow H_2$ system

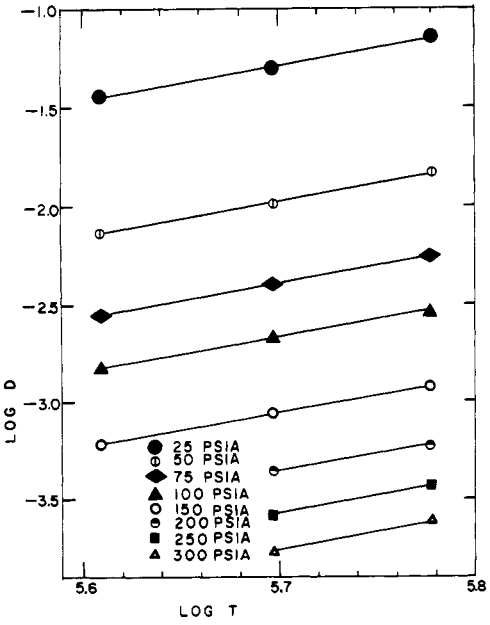

Figure 5. Isobaric behavior of diffusivity. Example shown for $C_3H_8^\infty \rightarrow H_2$ system

should be obtained between the two methods; the results of this study are summarized in Tables III-VII. The detailed example in Table III is representative of the basic experimental data. The standard deviation of this example for the 12 single flow rate diffusivities is ±0.0004. The basic experimental data are recorded in the thesis (*13*).

Typical plots of the data are shown in Figures 3-5. All of the systems showed the density-diffusivity products to be independent of the density for the range of this investigation (Figure 3). One example of the multiflow rate calculation is shown in Figure 4 for the radioactive system. As shown in Figure 5, the systems exhibited linear behavior on an isobaric plot of log *D* vs. log absolute temperature.

Acknowledgment

The late Walter E. A. Ruska was responsible for the design of the ionization chamber, the radioactive sample pump reservoir, and the high-pressure injection valve. The construction and assistance of Ray Martin and James Chappel of the University Machine Shop and of George Shamblin and Bill Peters of the University Electronics Shop are greatly appreciated. The Union Carbide Chemical Corp. provided the silicone bath liquids. The Phillips Petroleum Co. provided the isohexane bath fluid and the research-grade gases C_2H_6, C_3H_8, and n-C_4H_{10}.

Literature Cited

(1) Ananthakrishnan, V., Gill, W. N., Barduhn, A. J., *AIChE J.*, **11**, 1063-72 (1965).
(2) Ananthakrishnan, V., Gill, W. N., Barduhn, A. J., *ibid.*, **12**, 906-15 (1966).
(3) Aris, R., *Proc. Roy. Soc. (London)*, **A235**, 67-77 (1956).
(4) Aris, R., *ibid.*, **A252**, 538-50 (1959).
(5) Aris, R., *Chem. Eng. Sci.*, **9**, 266-67 (1959).
(6) Balenovic, Z., Myers, M. N., Giddings, J. C., *J. Chem Phys.*, **52**, 915-22 (1970).
(7) Bischoff, K. B., *Chem. Eng. Sci.*, **12**, 69-70 (1960).
(8) Bischoff, K. B., Levenspiel, O., *ibid.*, **17**, 245-55 (1962).
(9) Bischoff, K. B., Levenspiel, O., *ibid.*, pp 257-64.
(10) Boyd, C. A., Stein, N., Steingrimsson, V., Rumpel, W. F., *J. Chem. Phys.*, **19**, 548-53 (1951).
(11) Chang, G. T., PhD thesis, Rice University, Houston, Tex., Jan. 1966.
(12) Chang, G. T., Kobayashi, R., XXXVIth International Congress on Industrial Chemistry, 9 pp. G. II.—S.4.—571, Brussels, Belgium, 1966.
(13) Chu, T.-C., PhD thesis, Rice University, Houston, Tex., August 1972.
(14) Chuang, S.-Y., PhD thesis, Rice University, Houston, Tex., April 1972.
(15) Fejes, P., Czárán, L., *Acta Chim. Hung. Tomus*, **29**, 171-87 (1961).
(16) Gill, W. N., Ananthakrishnan, V., *AIChE J.*, **13**, 801-07 (1967).
(17) Hu, A. T., PhD thesis, Rice University, Houston, Tex., May 1969.
(18) Hu, A. T., Kobayashi, R., *J. Chem. Eng. Data*, **15**, 328-35 (1970).
(19) Knox, J. H., McLaren, L., *Anal. Chem.*, **36**, 1477-82 (1964).
(20) Koutsky, J. A., Adler, R. J., *Can. J. Chem. Eng.*, **42**, 239-46 (1964).
(21) van der Laan, E. Th., *Chem. Eng. Sci.*, **7**, 187-91 (1958).
(22) Liner, J. C., Weissman, S., *J. Chem. Phys.*, **56**, 2288-90 (1972).
(23) Loschmidt, J., *Sitzungsber. Akad. Wiss. Wien, Math. Naturwiss. Kl., Abt. II*, **61**, 367-80 (1870).
(24) Obermayer, A. V., *ibid.*, **81**, 1102-27 (1880).
(25) Strehlow, R. A., *J. Chem. Phys.*, **21**, 2101-06 (1953).
(26) Taylor, G., *Proc. Roy. Soc.*, (London), **A219**, 186-203 (1953).
(27) Taylor, G., *ibid.*, **A225**, 473-77 (1954).
(28) Walker, R. E., Westenberg, A. A., *J. Chem. Phys.*, **29**, 1139-46 (1958).
(29) Walker, R. E., Westenberg, A. A., *ibid.*, pp 1147-53.
(30) Walker, R. E., deHaas, N., Westenberg, A. A., *ibid.*, **32**, 1314-16 (1960).

Received for review February 13, 1974. Accepted June 17, 1974. Financial support was provided by the National Science Foundation and Columbia Gas Systems Service Corp.

Dielectric Constants, Viscosities, and Related Physical Properties of Four Liquid Pyridine–*N*-Oxides at Several Temperatures

Jerry F. Casteel and Paul G. Sears[1]
Department of Chemistry, University of Kentucky, Lexington, Ky. 40506

Dielectric constants, viscosities, densities, and refractive indices of four liquid pyridine–*N*-oxides, were measured at several temperatures ranging from 25° to 125°C. The experimental data as functions of temperature were fitted precisely to appropriate equations. Values of activation energies of viscous flow and Kirkwood correlation factors were also calculated. At comparable temperatures, the dielectric constants and viscosities of the pyridine–*N*-oxides were significantly affected by the position of the methyl group. The viscosity also tended to increase as the molecular weight decreased. The Kirkwood correlation factors ranged from 0.65 to 1.21, implying only slight amounts of net parallel or antiparallel configurations of dipoles in the liquids.

Pyridine–*N*-oxides and other aromatic amine oxides have been studied extensively since about 1940, and their preparations, properties, and chemistry have been reviewed comprehensively by Ochiai (*18*). During the last five years, there has been an unusually large number of articles dealing with aromatic–*N*-oxides as ligands in metal complexes (*2, 8–10, 26*).

Several pyridine–*N*-oxides are now commercially available. At least three of these highly polar compounds have melting points below 50°C and may possibly represent a new type of useful nonaqueous solvent. Although the pyridine–*N*-oxides have received considerable attention from both organic and inorganic chemists, the literature contains a paucity of data concerning the physical properties of these compounds as highly purified liquids. This study, therefore, was undertaken to determine the dielectric constants, viscosities, and other physical properties of pyridine–*N*-oxide and three of its methyl derivatives as functions of temperature.

Experimental

Pyridine–*N*-oxide (PO), 2-methylpyridine–*N*-oxide (2MPO), 3-methylpyridine–*N*-oxide (3MPO), and 2,6-dimethylpyridine–*N*-oxide (2,6DMPO) were obtained from the Reilly Tar and Chemical Corp. The *N*-oxides were

---

[1] To whom correspondence should be addressed.